



Ground motion directionality effects on inelastic spectral displacements

Savvinos Aristeidou - PhD Candidate, Scuola Universitaria Superiore IUSS di Pavia, Italy, e-mail: savvinos.aristeidou@iusspavia.it

Karim Tarbali - Research Fellow, The University of Edinburgh, Edinburgh, United Kingdom, e-mail: karim.tarbali@ed.ac.uk

Gerard J. O'Reilly - Assistant Professor, Scuola Universitaria Superiore IUSS di Pavia, Italy, e-mail: gerard.oreilly@iusspavia.it

Abstract: This paper investigates the effect of ground motion (GM) directionality on the non-linear response of bilinear single-degree-of-freedom (SDOF) systems, utilising a subset of the NGA-West2 database. The aim is to highlight the general trends in the median, *RotD50*, and maximum, *RotD100*, directional response. A parametric study was carried out by varying the force reduction factor, R , and the initial elastic period, T_{el} , of many SDOF systems for a wide range of causal parameters (M_w , R_{rup} & $V_{s,30}$). By examining the results for various levels of R and highly ductile response, systems with short T_{el} tended to exhibit relatively low response directionality, whereas long T_{el} systems showed relatively high response directionality. Considering all the SDOF systems analysed, the ones that exhibited the highest directionality effects were the systems with short T_{el} and low R . Comparison with classic R - μ - T relationships available in the literature illustrated the notable impacts of directionality on non-linear response quantification. By binning the causal parameters and separating the near- and far-fault GMs, it was possible to determine the more salient directionality effects of near-fault GMs, when compared with far-fault GMs on the non-linear systems.

Keywords: directionality; non-linear response; bilinear SDOF; *RotD50*; *RotD100*

1. Introduction

An accurate representation of damage in the urbanised area is needed for disaster risk assessment and urban planning. This requires appropriate ground motion (GM) severity measures that characterise the realistic response of non-linear (NL) systems and account for their maximum directional response. Since earthquake-induced GMs are felt principally as shaking in three dimensions (i.e., three translational and three rotational components), there is a need to consider the different possible incidence angles in which the propagating seismic waves can affect engineered systems. Earthquake hazard and structural response analysis are often combined using an intensity measure (IM) (Bradley 2012), which connects the structural response thresholds to the distribution of GM intensities required to exceed them. The most common IM used in building codes and seismic response analysis methods is the spectral acceleration at a given period T of vibration, $Sa(T)$. In this paper, the notation Sa will be used for brevity, implying that it refers to the spectral acceleration at a period T and 5% of critical damping.

Given that structures are 3D objects that can be excited in multiple directions by ground shaking, a question that has often arisen when defining Sa is: in which orientation should it be defined? Baker and Cornell (2006) addressed this question by demonstrating the consistent use of spectral acceleration of an arbitrary component, Sa_{arb} , and the geometric mean of spectral acceleration of the two as-recorded components, Sa_{gm} , in probabilistic seismic analyses. In the last decades, various definitions have been proposed to compute a

Sa measure that may be considered an appropriate IM of the ground motion in the 2D horizontal plane. Some of these definitions include the geometric mean of the Sa in the two as-recorded directions, the median or maximum value of response spectra over all orientations (Boore et al. 2006; Boore 2010). Boore (2010) defines $RotDnn$ as the nn^{th} percentile of all rotation angles sorted by amplitude at each period, with D denoting the period-dependent rotation angle. In this paper, these Sa (or displacement) definitions (i.e., $RotD100$, $RotD50$ and $RotD00$) were used to quantify the directional response of both bilinear and linear SDOF oscillators.

To date, the efforts in the literature have considered bidirectional or multi-directional response of either linear-elastic systems or complex non-linear structural systems (Nievas and Sullivan 2017; Feng et al. 2018; Pinzon et al. 2019; etc.). On the one hand, many inspiring insights have been obtained from previous studies on linear systems. However, the focus of this study was to extend such efforts to NL systems. On the other hand, although the studies examining complex NL systems give interesting conclusions, most are structure-specific applications. In contrast, the general trends of the phenomenon were explored here. Therefore, there is a need to better understand the trend in the NL directional response of simple bilinear systems and evaluate whether the trends observed on linear systems are still valid or somehow correlated. Several researchers have also developed GM models for peak inelastic displacements of single-degree-of-freedom (SDOF) systems, Sd_i , (Huang et al. 2020; Heresi et al. 2018). Sd_i can be an effective IM relating the ground motion intensity with the inelastic response and, therefore, the structural and non-structural damage of engineered systems (Stafford et al. 2016). Using Sd_i , instead of elastic Sa can result in improved seismic-demand predictions, subsequent damage and loss estimates for multi-degree-of-freedom structures (O'Reilly et al. 2020).

In this study, the $RotDnn$ for the 00th, 50th and 100th period-dependent percentile of Sd_i was calculated for all non-redundant incidence angles for bilinear SDOF systems with a range of elastic periods, T_{el} , and force reduction factors, R . The goal was to understand the directionality effects of GMs of various characteristics on inelastic systems, as an extension from previously examined elastic systems (Shahi and Baker 2014). All in all, this study is useful because it provides insights into the maximum directional response of NL systems, which can enable a more comprehensive quantification of damage in engineered systems.

2. Methodology

A flowchart of the steps followed to obtain the peak inelastic displacement response for each GM and rotation angle is given in Figure 1. Firstly, the GMs within the range of M_w and R_{rup} of interest were extracted from the NGA-West2 database, which is described in Section 2.1. Then, the range of R and T_{el} values, along with the hysteretic behaviour, the post-yield stiffness, and the damping of the system, were defined. It is noted that the R assigned to the system was one per GM and kept constant over the different rotation angles of that GM. This was chosen to be based on the linear-elastic $RotD100$ response. Then the ground motions were rotated and applied to the NL system to obtain the maximum displacement of the oscillator per GM per rotation angle. The elastic $Sa_{RotD100}$ and Sa_{RotD50} were obtained from the meta-data in the flatfile of the NGA-West2 database. It is worth recalling that Sa and Sd can be used interchangeably for elastic systems, whereas for inelastic systems, the Sd_i is more appropriate in characterising their response. The total number of analyses presented in this study amounted to $7167 \text{ GMs} \times 5 R \times 10 T_{el} \times 30 \text{ incidence angles} = 10,750,500$ inelastic SDOF analyses.

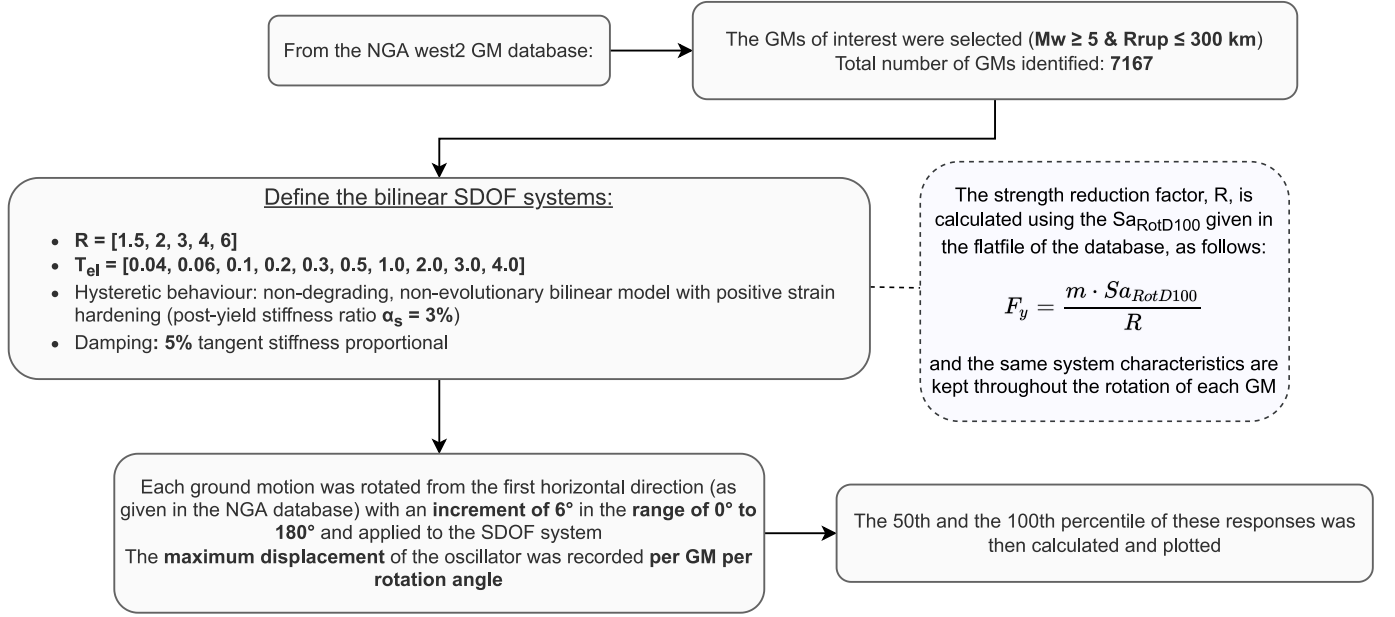


Figure 1. Computational workflow

2.1. Ground motion database

The NGA-West2 database (Ancheta et al. 2013) is a comprehensive database of shallow crustal earthquakes in active tectonic regions. From the whole database, a subset of GMs that can cause structural or non-structural damage, depending on magnitude and distance, was selected for the analyses; specifically, the subset considered was $M_w \geq 5$ and $R_{rup} \leq 300$ km. The considered GMs distributed in the M_w - R_{rup} ranges are shown in Figure 2(a). This subset includes 7167 GMs, whose scatter plot of distance, magnitude and $V_{s,30}$ is depicted in Figure 2(b). Additionally, GMs with the ‘maximum usable period’ (calculated from the lowest usable frequency given in the flatfile) lower than the elastic period of the system were filtered out of the considered GM subset.

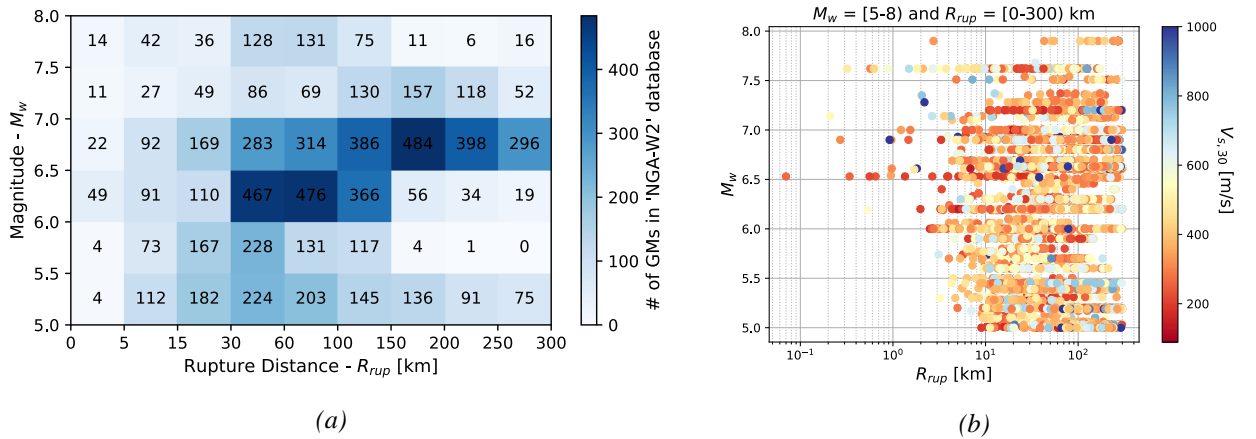


Figure 2. (a) M_w - R_{rup} bins, and (b) M_w - R_{rup} scatter plot, with the $V_{s,30}$ distribution of the considered GMs

2.2. Description of the considered SDOF system

The inelastic SDOF system chosen for this study was a simple bilinear model with a positive strain hardening (i.e., post-yield stiffness ratio $\alpha_s = 3\%$), as shown in Figure 3. The hysteretic behaviour of this system is non-degrading and non-evolutionary. A tangent stiffness proportional damping model was adopted with a ratio of $\xi = 5\%$, as it was shown to be

appropriate for inelastic response history analyses (Petrini et al. 2008). Future work may consider the response of hysteretic models representative of different structural systems.

The set of examined elastic periods was $T_{el} = [0.04, 0.06, 0.1, 0.2, 0.3, 0.5, 1.0, 2.0, 3.0, 4.0]$ in seconds, and the strength reduction factors was $R = [1.5, 2, 3, 4, 6]$, which are both shown in Figure 1. R was defined as the ratio of maximum force demand of the elastic system subjected to a given ground motion, F_{el} , to the assigned SDOF yield strength, F_y .

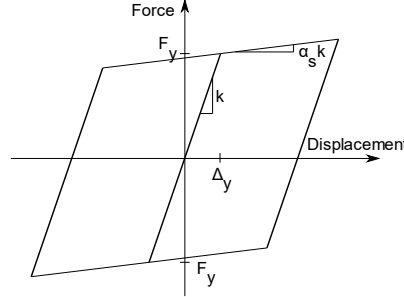


Figure 3. Hysteretic model of the bilinear SDOF oscillator

3. Results

3.1. $Sd_{i, RotDnn}$ spectra

The 84th, 50th and 16th percentiles of the elastic, $Sd_{e, RotDnn}$, and inelastic, $Sd_{i, RotDnn}$, spectral displacements for the considered GMs are shown in Figure 4. The *RotD00* (i.e., the minimum directional response) of the inelastic response is also considered in the comparisons. Generally, it can be seen from Figure 4(a) and (b) that, for $T_{el} < 1$ s, the median Sd_i increases with an increase in R , while for $T_{el} > 1$ s the inelastic response is almost the same as the elastic one across all the different R factors. This result was expected, as the non-linear behaviour of medium to long-period structures typically follows the equal-displacements rule. In contrast, short-period structures typically follow the equal-energy rule (Chopra 2014). This held for different inelastic responses quantities *RotDnn* and was also presented in (Huang et al. 2020).

Figure 4(c) compares the *RotD50* elastic displacement spectrum with the *RotD00* of the inelastic displacement spectrum. This was to investigate whether the elastic *RotD50* response, conventionally used in the seismic design process, can be higher than the minimum inelastic response. It is interesting to see that even the 00th percentile of inelastic displacement can be higher than the 50th percentile of elastic displacement for periods shorter than $T_{el} = 0.3$ s and high R factors. While for longer periods, the aforementioned inelastic response is always lower than the elastic one. For R equal to 1.5, the inelastic response is almost in any case lower than the elastic one. This shows that the elastic response cannot be sufficient in representing the minimum directional response of inelastic systems with short T_{el} .

3.2. Directionality measure

The most widespread measure to describe the GM directionality is the *RotD100/RotD50* ratio and it was the one utilised herein. Figure 5(a) shows the median directionality measure for the inelastic and elastic (i.e., $R=1$) systems and compares them with the corresponding geometric mean values of Shahi and Baker (2014) for an elastic response. Firstly, it can be seen that the elastic directionality measure for the selected range of GM causal parameters is in good agreement with the model developed by Shahi and Baker (2014). In the case of elastic systems, the ratio of $Sa_{RotD100}$ to Sa_{RotD50} ranges from 1 to $\sqrt{2}$ for the case of unpolarised to extremely polarised, respectively. However, this directionality measure can

take much higher values for an inelastic system with the lower bound staying the same. Figure 5(a) shows that, for $T_{el} > 0.3s$, the directionality measure increases as the R increases. Also, regardless of the R value, all the directionality measures move closer to the elastic one for periods larger than $0.5s$. However, for $T_{el} < 0.3s$, the systems with lower R factors start to exhibit a more pronounced directionality effect.

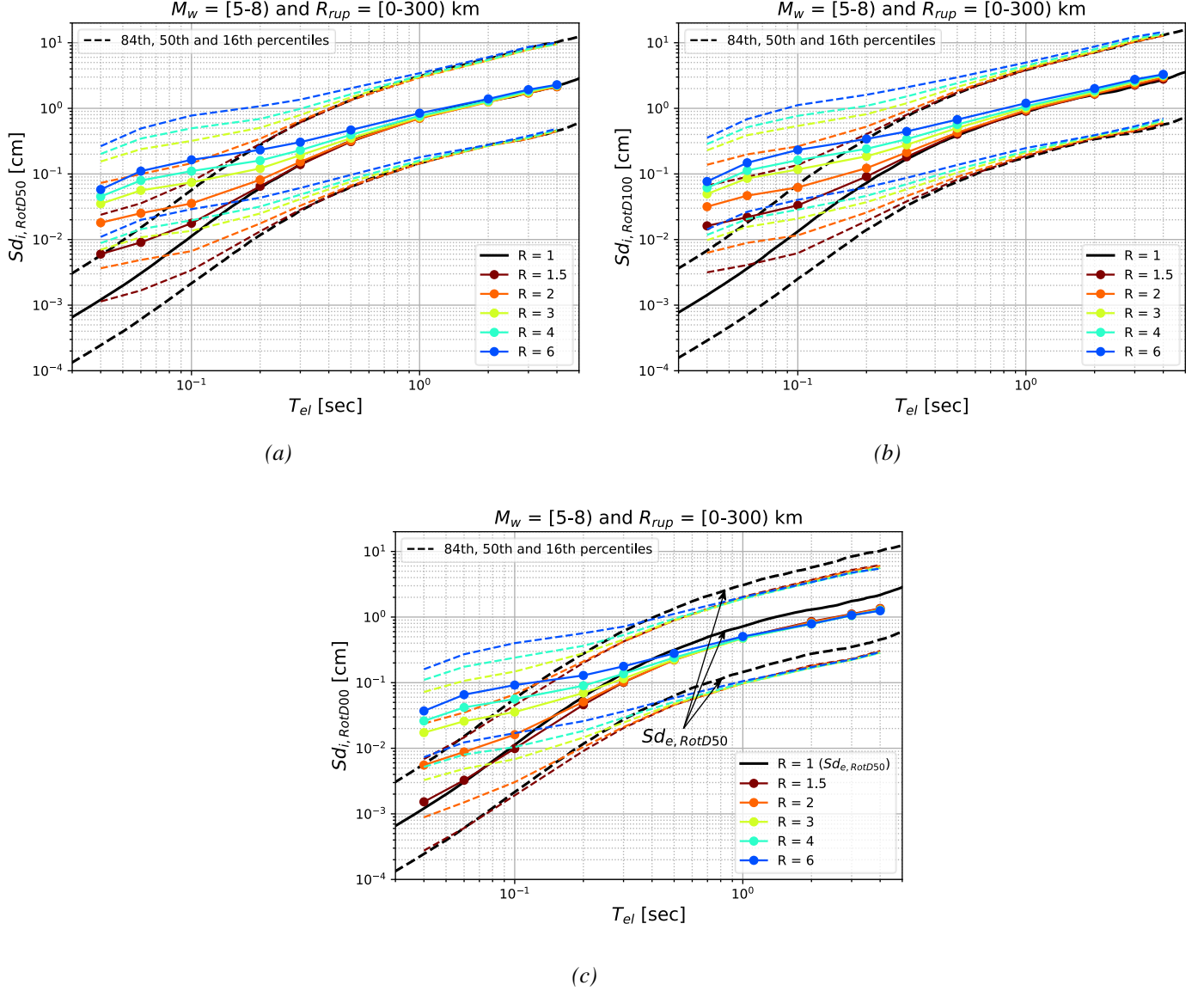


Figure 4. Median Sd_i spectra for (a) RotD50; (b) RotD100; and (c) RotD00 along with the RotD50 elastic displacement spectrum of the elastic system

The dispersion of the directionality measure, calculated as the standard deviation of the natural logarithm of the directionality measure, is presented in Figure 5(b), where it can be seen that the overall trend matches the median values. In other words, there is also high dispersion for the inelastic systems with high median values. The dispersion is minimised and approaches the dispersion of the elastic system for long T_{el} . Note also that the dispersion of the elastic system matches the one given in Shahi and Baker (2014) quite well.

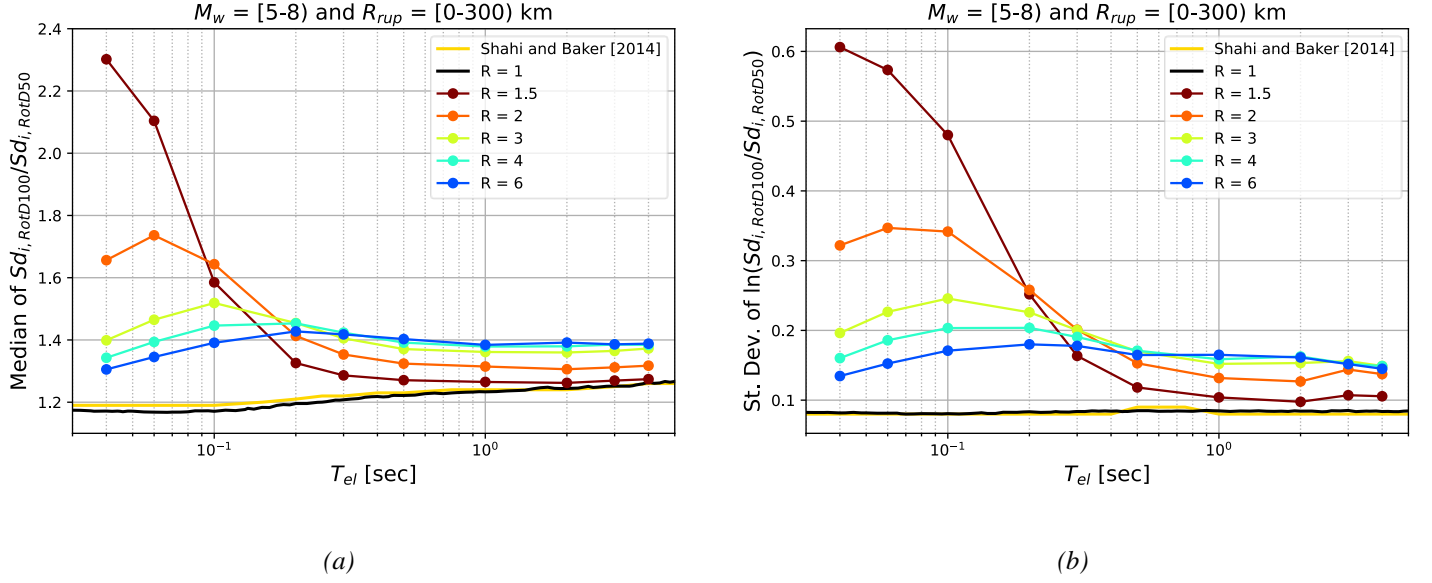


Figure 5. Directionality measure: (a) median $Sd_{i,RotD100}/Sd_{i,RotD50}$; and (b) dispersion of $Sd_{i,RotD100}/Sd_{i,RotD50}$ for the different T_{el} and R factors

3.3. Maximum displacement ductility

Figure 6 depicts the median displacement ductility, μ , calculated as $Sd_{i,RotD100}/\Delta_y$ for the considered T_{el} and R factors. It can be seen that, for the same R factor of the system, the μ decreases as T_{el} increases until it generally plateaus for $T_{el} > 2$ s. This is essentially due to the non-linear behaviour of the systems converging towards the equal-displacement rule. Two well-established models relating R , μ and T_{el} from the literature, Nassar and Krawinkler (1991) and Vidic et al. (1994), were also plotted in Figure 6 for comparison. It can be seen that the trend of those models is in good agreement with the trend of the results obtained here. Nonetheless, the median values estimated in this study are somewhat higher, especially for the systems with high R factors and short T_{el} . This is due to several reasons. Firstly, the ductility presented here is for the system's response under the GM rotated to the direction of 100th percentile linear-elastic response. At the same time, the other studies were performed for the two as-recorded components of GMs. Secondly, although both previous studies used bilinear hysteretic models, there are slight differences in the post-yield stiffness and the assumption of viscous damping modelling. Furthermore, Nassar and Krawinkler (1991) considered 15 GMs in the Western United States and Vidic et al. (1994) considered 20 GMs recorded in the Western United States and the 1979 Montenegro, Yugoslavia earthquake, as opposed to the 7167 GMs considered in this study.

3.4. Directionality in near- and far-fault ground motions

Different bins of near-fault and far-fault GMs were examined in terms of the directional inelastic response and directionality measures, depicted in Figure 7. From the inelastic spectrum, it can be seen that near-fault GMs result in higher elastic and inelastic displacements for the entire range of T_{el} . It is also apparent that the near-fault GMs result in higher directionality measure (i.e., $Sd_{i,RotD100}/Sd_{i,RotD50}$), as it is well known that near-fault GMs exhibit higher directional effects (Bray and Rodriguez-Marek 2004; Huang et al. 2009; Tarbali 2017). A similar trend is also present for the directionality measure presented in Figure 7(c).

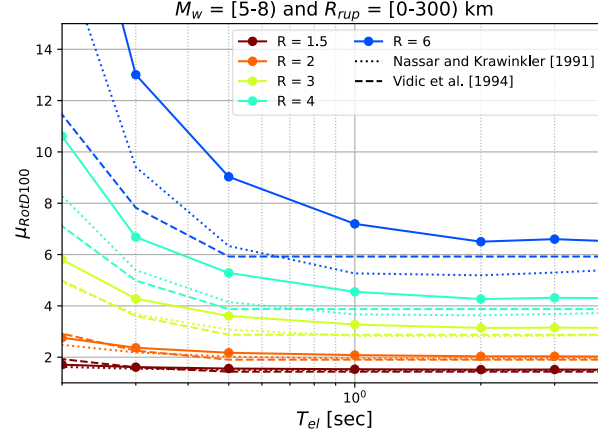
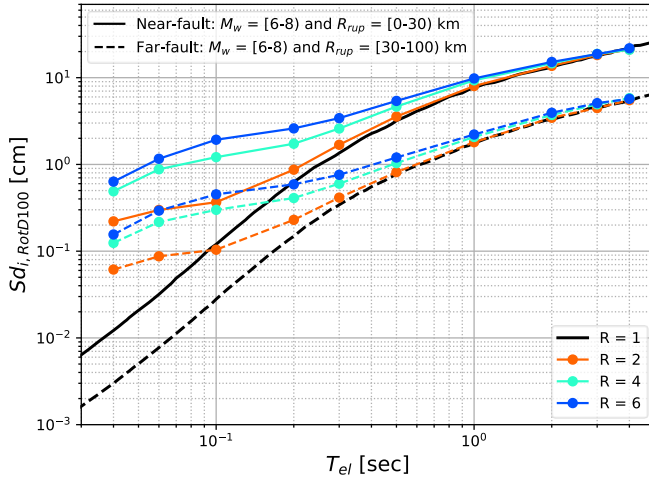
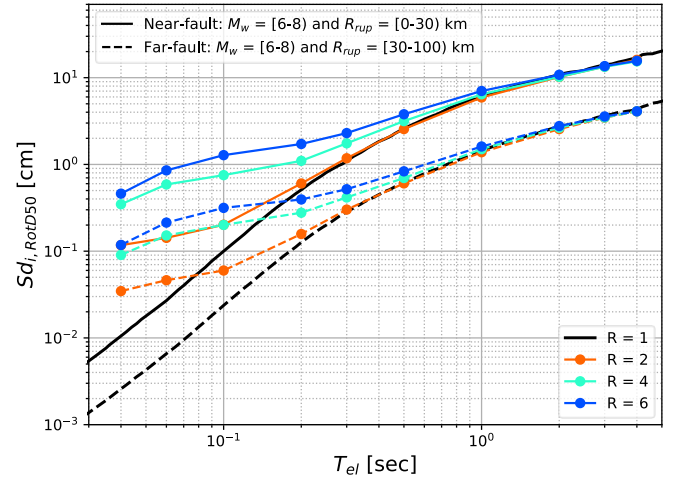


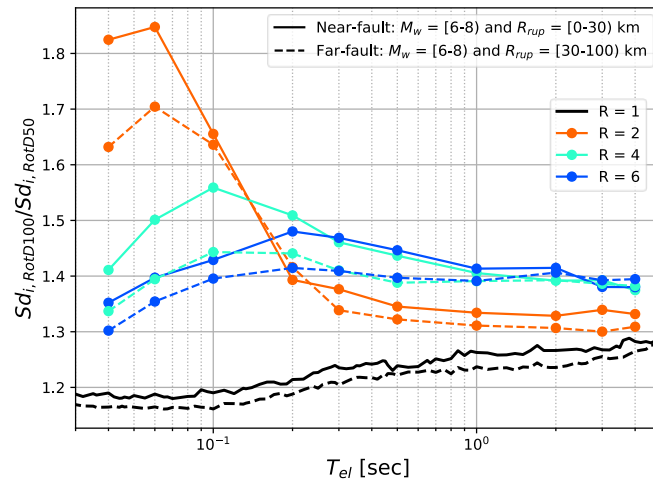
Figure 6. Displacement ductility in the 100th percentile of the response versus period and reduction factor and compared with two conventional models



(a)



(b)



(c)

Figure 7. (a) Median $Sd_{i,RotD100}$ spectra, (b) median $Sd_{i,RotD50}$ spectra and (c) median directionality measure ($Sd_{i,RotD100}/Sd_{i,RotD50}$) for near- and far-fault ground motions.

4. Summary

This paper examined the directionality of the ground motions in the NGA-West2 database for a range of inelastic SDOF systems. A bilinear hysteretic behaviour was chosen with varying elastic vibration period, T_{el} , and force reduction factor, R . The inelastic displacement spectra were computed for *RotD100*, *RotD50* and *RotD00* definitions and plotted against the corresponding elastic ones. These spectra provided insights on the response directionality of inelastic systems and their relationship with the elastic ones regarding peak spectral displacements. It was shown that the effect of directionality on the inelastic systems, quantified via the *RotD100/RotD50* ratio, increases with R for $T_{el} > 0.3s$, whereas the opposite trend was observed for $T_{el} < 0.3s$. Differences and impacts of considering directionality compared to traditional non-linear response models were also shown. Similarly, a subset of near-fault ground motions showed higher elastic and inelastic displacements and higher directionality for the entire range of T_{el} .

There are, nevertheless, some limitations and planned future developments stemming from this study. In particular, further studies will be performed using different hysteretic models (e.g., Ibarra-Medina-Krawinkler deterioration model) with different post-yield behaviours (e.g., negative post-yield stiffness). Additionally, the analyses will be extended to full 3D buildings or bridge structures. Lastly, similar analyses will be conducted for ground motions from subduction earthquakes, given the inherent differences in their duration and cumulative measures compared with shallow-crustal ground motions.

Acknowledgements

The work presented in this paper has been developed within the framework of the project "Dipartimenti di Eccellenza", funded by the Italian Ministry of Education, University and Research at IUSS Pavia.

References

- Ancheta, TD, RB Darragh, JP Stewart, E Seyhan, WJ Silva, BSJ Chiou, KE Wooddell, et al. 2013. "PEER NGA-West2 Database, Technical Report PEER 2013/03."
- Baker, Jack W., and C. Allin Cornell. 2006. "Which Spectral Acceleration Are You Using?" *Earthquake Spectra* 22 (2): 293–312. <https://doi.org/10.1193/1.2191540>.
- Boore, David M. 2010. "Orientation-Independent, Nongeometric-Mean Measures of Seismic Intensity from Two Horizontal Components of Motion." *Bulletin of the Seismological Society of America* 100 (4): 1830–35. <https://doi.org/10.1785/0120090400>.
- Boore, David M., Jennie Watson-Lamprey, and Norman A. Abrahamson. 2006. "Orientation-Independent Measures of Ground Motion." *Bulletin of the Seismological Society of America* 96 (4 A): 1502–11. <https://doi.org/10.1785/0120050209>.
- Bradley, Brendon A. 2012. "The Seismic Demand Hazard and Importance of the Conditioning Intensity Measure." *Earthquake Engineering & Structural Dynamics* 41 (11): 1417–37. <https://doi.org/10.1002/eqe.2221>.
- Bray, Jonathan D., and Adrian Rodriguez-Marek. 2004. "Characterization of Forward-Directivity Ground Motions in the near-Fault Region." *Soil Dynamics and Earthquake Engineering* 24 (11): 815–28. <https://doi.org/10.1016/j.soildyn.2004.05.001>.
- Chopra, Anil K. 2014. *Dynamics of Structures - Theory and Applications to Earthquake*

Engineering. Fourth Ed. Harlow: Pearson Education Limited.

- Feng, Ruiwei, Xiaowei Wang, Wancheng Yuan, and Juanya Yu. 2018. "Impact of Seismic Excitation Direction on the Fragility Analysis of Horizontally Curved Concrete Bridges." *Bulletin of Earthquake Engineering* 16 (10): 4705–33. <https://doi.org/10.1007/s10518-018-0400-2>.
- Heresi, Pablo, Héctor Dávalos, and Eduardo Miranda. 2018. "Ground Motion Prediction Model for the Peak Inelastic Displacement of Single-Degree-of-Freedom Bilinear Systems." *Earthquake Spectra* 34 (3): 1177–99. <https://doi.org/10.1193/061517EQS118M>.
- Huang, Chen, Karim Tarbali, and Carmine Galasso. 2020. "A Region-Specific Ground-Motion Model for Inelastic Spectral Displacement in Northern Italy Considering Spatial Correlation Properties." *Seismological Research Letters* 92 (3): 1979–91. <https://doi.org/10.1785/0220200249>.
- Huang, Yin Nan, Andrew S. Whittaker, and Nicolas Luco. 2009. "Orientation of Maximum Spectral Demand in the Near-Fault Region." *Earthquake Spectra* 25 (3): 707–17. <https://doi.org/10.1193/1.3158997>.
- Nassar, Aladdin Aly, and Helmut Krawinkler. 1991. "Seismic Demands for SDOF and MDOF Systems, Report No. 95." *Stanford University*, no. 95: 204.
- Nievas, Cecilia I., and Timothy J. Sullivan. 2017. "Accounting for Directionality as a Function of Structural Typology in Performance-Based Earthquake Engineering Design." *Earthquake Engineering and Structural Dynamics* 46 (5): 791–809. <https://doi.org/10.1002/eqe.2831>.
- O'Reilly, Gerard J., Ricardo Monteiro, Al Mouayed Bellah Nafeh, Timothy J. Sullivan, and Gian Michele Calvi. 2020. "Displacement-Based Framework for Simplified Seismic Loss Assessment." *Journal of Earthquake Engineering* 24 (sup1): 1–22. <https://doi.org/10.1080/13632469.2020.1730272>.
- Petrini, Lorenza, Claudio Maggi, M. J. Nigel Priestley, and G. Michele Calvi. 2008. "Experimental Verification of Viscous Damping Modeling for Inelastic Time History Analyses." *Journal of Earthquake Engineering* 12 (SUPPL. 1): 125–45. <https://doi.org/10.1080/13632460801925822>.
- Pinzon, Luis Alejandro, Sergio Alberto Diaz, Lluís G. Pujades, and Yeudy Felipe Vargas. 2019. "An Efficient Method for Considering the Directionality Effect of Earthquakes on Structures." *Journal of Earthquake Engineering* 25 (9): 1679–1708. <https://doi.org/10.1080/13632469.2019.1597783>.
- Shahi, Shrey K., and Jack W. Baker. 2014. "NGA-West2 Models for Ground Motion Directionality." *Earthquake Spectra* 30 (3): 1285–1300. <https://doi.org/10.1193/040913EQS097M>.
- Stafford, Peter J., Timothy J. Sullivan, and Domenico Pennucci. 2016. "Empirical Correlation between Inelastic and Elastic Spectral Displacement Demands." *Earthquake Spectra* 32 (3): 1419–48. <https://doi.org/10.1193/020515EQS021M>.
- Tarbali, Karim. 2017. "Ground Motion Selection for Seismic Response Analysis." PhD. dissertation, University of Canterbury.
- Vidic, Tomaž, Peter Fajfar, and Matej Fischinger. 1994. "Consistent Inelastic Design Spectra: Strength and Displacement." *Earthquake Engineering & Structural Dynamics* 23 (5): 507–21. <https://doi.org/10.1002/eqe.4290230504>.